

The Influence of Injection Timing on Combustion and Emission Characteristics of HSDI Diesel Engine

Hayder A. Dhahad

Machines & Equipment Engineering Department, University of Technology / Baghdad.
Email: hayder_abed2002@yahoo.com

Dr. Mohammed A. Abdulhadi

Machines & Equipment Engineering Department, University of Technology / Baghdad.

Dr. Ekhlas M. Alfayydh

Machines & Equipment Engineering Department, University of Technology / Baghdad.

Dr. T. Megaritis

Brunel University, UK

Received on: 2/10/2013 & Accepted on: 6/4/2014

ABSTRACT

An attempt has been made to study the combustion and emission characteristics of ultra-low diesel fuel for high speed direct injection (HSDI) diesel engine at different fuel injection timings(-12,-9,-6,-3,0)ATDC . The fuel injection pressure was 800 bar and at high load (80Nm= 5BMAP) , low load (40Nm=2.5BMAP) , With constant engine speed (1500rpm) . In-cylinder pressure was measured and then analyzes this pressure using LABVIWE program and calculation program in MATLAB software to extract the apparent heat release rate, the ignition delay, combustion duration and the amount of heat released during the premixed and diffusion combustion phases . The influence of injection timing on the exhaust emissions such as carbon monoxide (CO), total hydrocarbons (THCs), nitric oxides (NOx), smoke number (SN) and fuel consumption were also investigated.

A result referring to that the retardation of the injection timing lead to increase the ignition delay and therefore the premixed burn fraction which plays a key role in the combustion and emission characteristics .this leads to change combustion mode to low temperature combustion at late injection timing.

Keywords: combustion, diesel engine, injection pressure, gases emissions.

تأثير توقيت الحقن على خصائص الاحتراق والانبعثات لمحرك ديزل مباشر الحقن عالي السرعة

الخلاصة:

هذا البحث دراسة لخصائص الاحتراق والانبعثات لوقود الديزل منخفض الكبريت باستخدام محرك ديزل عالي السرعة وحقن مباشر ومع تغيير توقيت الحقن عند (0,-3,-6,-9,-12 ATDC), ضغط الحقن للوقود كان 800bar واجريت التجارب عند الحمل العالي (80Nm=5BMEP) والحمل المنخفض (40Nm=2.5BMEP), تم تثبيت سرعة المحرك عند 1500 rpm. تم قياس الضغط داخل غرفة الاحتراق ومن ثم تحليل هذا الضغط باستخدام برنامج LABVIWE وبرنامج حسابي باستخدام برنامج MATLAB لحساب معدل الحرارة المنطلقة وتأخر الاشتعال ومدة الاحتراق وكمية الحرارة المنطلقة فيطور الاحتراق المسبق الخلط وكذلك فيطور الاحتراق الانتشاري. تأثير توقيت الحقن على انبعاث الغازات العادم مثل اول اوكسيد الكربون (CO) الهادر وكابون غير المحترق الكلي (THC) واكاسيد الناتروجين (NOx) ورقم الدخان (SN) ومعدل استهلاك. النتائج اشارة الى ان تاخير توقيت الحقن يؤدي الى زيادة تاخير الاشتعال وبالتالي زيادة كمية

الاحتراق المسبق الخلط والذي يلعب الدور الرئيسي في تحديد خصائص الاحتراق والانبعاثات . وذلك يمكن ان يؤدي التغيرات طبيعة الاحتراق الى احتراق منخفض درجة الحرارة عندما يكون توقيت الحقن متاخر.

INTRODUCTION

The concern surrounding NO_x emissions in particular comes as a result of the role that they play in the formation of acid rain, ground-level ozone (a component of photochemical smog) and other air toxicity concerns [1,2]. The term 'NO_x' encompasses all oxides of nitrogen, but engine-out NO_x emissions are comprised in the largest part of NO, and the remainder is almost all NO₂, with only trace quantities of other molecules such as N₂O being emitted[3]. The formation of NO_x occurs through several main mechanisms. In a diesel engine, the extended Zeldovich or thermal mechanism is generally considered to be dominant [4]. The thermal mechanism is a temperature dependent process; formation rates become increasingly significant past approximately 1800 K, but beneath that, they are relatively low [5,6] As well as being influenced by temperature changes, thermal NO_x is dependent upon mixture stoichiometry and high-temperature residence times[7]. Although thermal NO_x formation is slow, formation rates can be increased by superequilibrium concentrations of the requisite radicals (as can be found in flame-fronts) and other faster acting NO_x formation mechanisms. Among these, the prompt NO route is most important, whereby NO_x is produced via hydrocarbon free radicals, primarily CH [8–11].

Soot is formed in the presence of a rich combustion where fuel pyrolysis, the process of hydrocarbon chain decomposition at elevated temperatures in the absence of oxygen, is likely to take place [12]; while, lubricating oil on the cylinder walls is also reported as a contributing factor [13]. Although the majority of the soot produced is oxidized during the combustion process, it remains the prime contaminant produced by diesel engines.

Soot formation has been extensively investigated with regard to combustion characteristics [14-18] and application of alternative fuels [19-21].

Recent studies on soot formation involved detailed analysis of the effect of alternative fuels [22-27], fuel injector nozzle design [28], fuel injection pressure [29,30], injection strategy [35,36], and Exhaust Gas Recirculation (EGR) [37-39]. Modifications of engine operating parameters through the application of the aforementioned techniques resulted in significant reduction in soot emission.

The effect of injection timing on diesel combustion efficiency and the soot-NO_x tradeoff is well established [31-34]. Injection timing is referenced with respect to TDC where injections before and after this reference are referred to as being advanced and retarded respectively.

The main focus of this work was to investigate the effects of fuel injection timing to understand the combustion and emission characteristics of ultra-low sulfur diesel fuel in a high speed direct injection diesel engine HSDI and that use of the modern fuel injection system type common rail injection system.

METHODOLOGY

Experimental setup and test conditions

Experiments were carried out in a 2.0 lit, 4 cylinders, 16 valves, and compression ratio 18.2, direct Injection Ford's Duratorq (Puma) Euro3 diesel engine. The engine was supplied by Ford as a prototype production unit which powered Ford Transits

and Mondeo cars. The engine is fully instrumented and coupled to a Schenck eddy current dynamometer. The schematic of the experimental setup is shown in Figure (1) and a photograph of the engine shown in the appendix A .

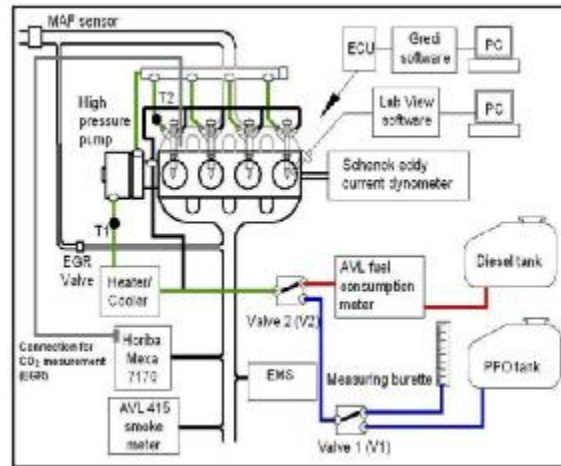


Figure (1). The schematic of experimental setup

In this investigation the engine was operated under naturally aspirated mode. The engine is fully instrumented, which enables the measurement of in-cylinder pressure and exhaust gas emissions under steady-state engine operating conditions. The in-cylinder pressures were measured using a Kistler pressure transducer fitted into the first cylinder of the engine a photograph of the pressure transducer shown in the appendix B. The signal from pressure transducer was amplified by the charge amplifier and then recorded by the Lab View software in conjunction with the shaft encoder. In-cylinder pressure data were collected over 100 engine cycles per measurement, and the measurement was repeated 5 times for each point in the experimental matrix. The in-cylinder pressure data was averaged from 100 cycles. Output from the Lab VIEW program are showed in Figure(2) .

A common rail fuel injection system with six holes injector of 0.154 mm in diameter each , and a spray-hole angle of 154 degree was used in this investigation.

The influence of injection timing has been tested. The Gredi software allowed the control and change of these parameters by programming the Electronic Control Unit ECU in real time. , injection timing could be directly controlled through the software. The gaseous exhaust emissions were acquired using a Horiba-Mexa 7170DEGR gas analyser. A non-dispersive infrared method has been used for measuring the CO and CO₂ emissions. The NO_x emissions have been measured using chemiluminescence technique whereas the total unburnt hydrocarbons (THC) were measured using the flame ionization detection technique, Figure 3 show sample of these measurements and a photograph of the Horiba-Mexa 7170DEGR gas analyser shown in the appendix C.

Emissions data were recorded over 180 s intervals, twice for each point in the experimental matrix. Again, this process was repeated for confirmatory purposes.

The engine exhaust smoke emissions were measured using the AVL – 415 smoke meter while the diesel fuel consumption was measured using an AVL fuel consumption meter, which is based on gravimetric measurement principle .

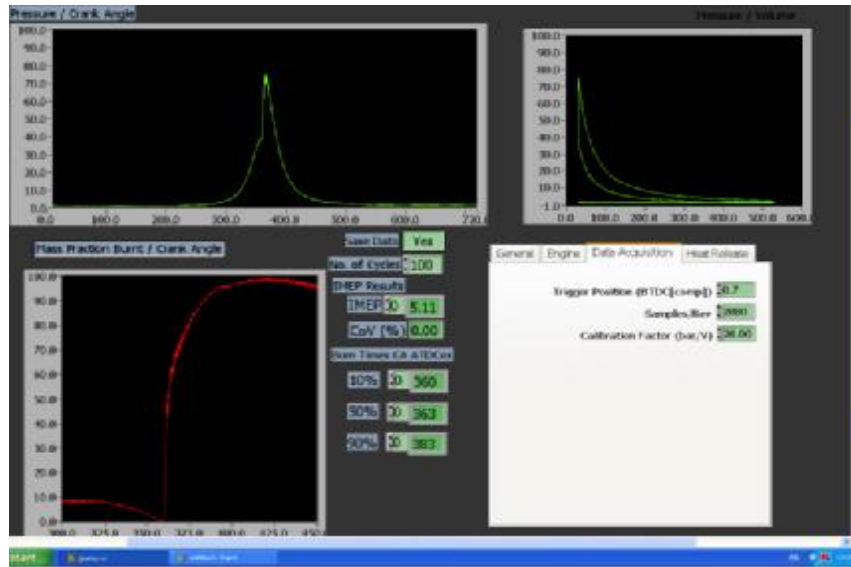


Figure (2) LabVIEW program screen

Measurements were carried out using the standard ultra-low sulfur diesel fuel. Table (1) provides an overview of all tested engine operating conditions .The load and speed conditions have been chosen to represent the commonly used operating condition for the stationary driving cycle for automotive diesel engines.

Table (1) Experiment matrix

| Load | Injection pressure bar | Engine speed rpm | Injection timing (ATDC) |
|-------------------------------|------------------------|------------------|-------------------------|
| 40 N.m = 2.5 bar (BMEP) | 800 | 1500 | -12 |
| | | | -9 |
| | | | -6 |
| | | | -3 |
| | | | 0 |
| 80 N.m =5 bar (BMEP) | | | -12 |
| | | | -9 |
| | | | -6 |
| | | | -3 |
| | | | 0 |



Figure. (3) Horiba measurement screen

After start-up, the engine was allowed to warm up until hydrocarbon emissions (the slowest pollutant to stabilize) had settled to an apparent steady state; this typically took around 90 min under an 80 Nm load. At each operational condition data collection was postponed until all emissions had reached apparent consistency when viewed over 180 s duration.

Data Analysis

Raw data collected using LabView was loaded into MATLAB and batch processed to retrieve the pertinent information. In-cylinder pressure was processed to extract relevant data-peak pressure, angle of peak pressure, angle between start of combustion (SOC) and peak pressure- and to calculate apparent heat release rate (AHRR) data using the traditional first law heat release model (19) without any modeling of heat transfer or crevice effects, and using an assumed constant specific heat ratio of 1.35. This is a very basic approach, but it is held to be sufficient for the purposes of comparison.

Approximations of C_p/C_v were made from the logarithm of pressure versus logarithm of volume charts in order to ensure that a constant value would represent fuel equally well. The calculated ratios of specific heats were found to be essentially consistent for ULSD under varying conditions, and so an assumed value of 1.35 was found to be adequate.

The definitions on which calculations of AHRR related parameters were based are illustrated in Figure (4) and explained in the accompanying text. Each 100 cycle pressure data set was used to generate a single average pressure trace, in order to reduce noise while maintaining the essential characteristics of combustion. It should also be noted that although pressure data was only logged by the data acquisition system once per crank angle degree, all values were interpolated to one decimal place

by the MATLAB code. All heat release parameters were calculated from the AHRR curve without filtering or averaging, except for the end of combustion, which was defined on the basis of the moving average of AHRR in order to improve consistency, and the end of premixed burn, which was calculated from the second derivative of AHRR, The following is a definition of the combustion characteristics in the fig.(4)

1. Start of injection (SOI) was defined from the commanded SOI set within the engine management software. Any potential difference between commanded and actual SOI, due to solenoid delay for instance, should be consistent between measurements, since engine speed was held constant.
2. Ignition delay (ID) was defined as the difference between commanded SOI and calculated SOC.
3. Start of combustion (SOC) was defined as the point at which the AHRR curve crossed the x axis; that is, the heat release rate became positive.
4. Premixed burn fraction (PMBF) was defined as the integral of the AHRR curve between SOC and EOPMB, divided by the integral of the AHRR curve between SOC and EOC.
5. End of premixed burn (EOPMB) was defined as the first point at which the second differential of heat release rate reached a local maximum following the global minimum. Under most conditions, this approximately corresponds to the position at which the AHRR reaches a first local minimum following the global maximum, but the second differential was used instead because under low loads there local minimum in the AHRR curve is not always clear, as can be seen in Figure 4.
6. End of combustion (EOC) was defined as the first point at which the moving average of heat release rate dropped below zero. A moving average was used to minimize problems due to noise, while still being representative of the general tendencies of the data.

Other values calculated from the in-cylinder pressure data including total apparent heat release, peak AHRR, PMBF, 10–90% burn fraction intervals, duration of partial burn fraction intervals, and average burn rates through partial intervals. Emissions data were averaged over the 180 s durations recorded.

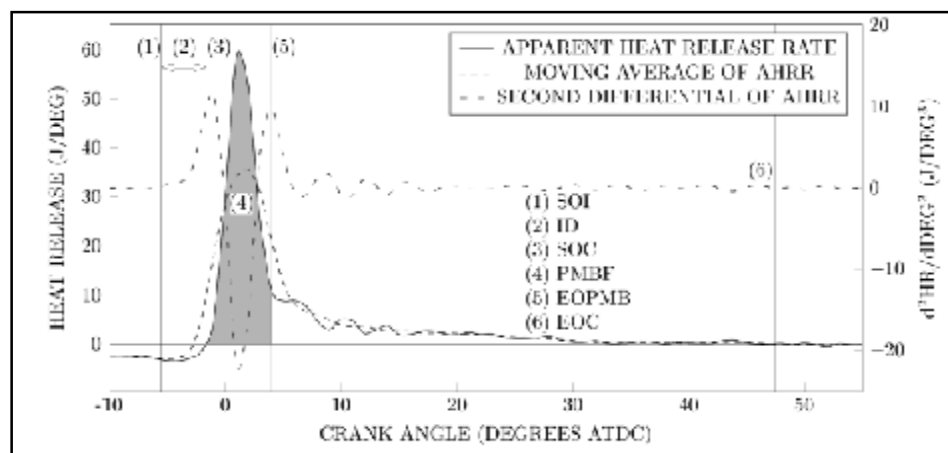


Figure (4). Labeled plot of heat release and the derivatives used to calculate combustion criteria

Results and Discussions

Combustion characteristics

Figure 5 shows the variations of the in-cylinder pressure with crank angle at high load (80 N.m= 5 bar BMEP) with variation of injection timing, we can clearly note that the value of the maximum pressure drop with the approach of injection timing to TDC , we also note the shift in the combustion phase and its corresponding pressure peaks .

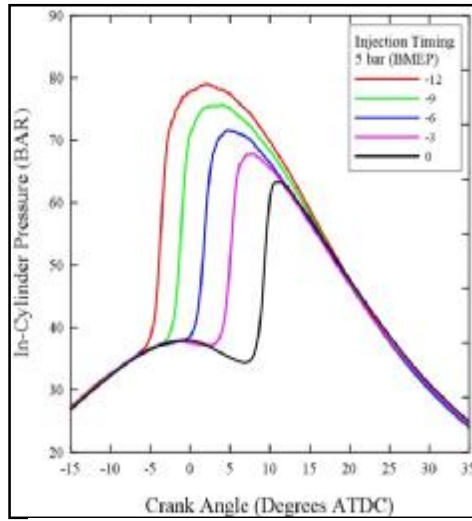


Figure.(5) In-cylinder pressure under 80Nm

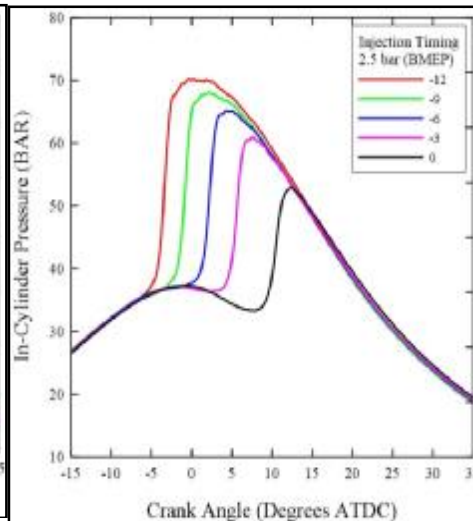


Figure.(6) In-cylinder pressure under 40Nm

Table (2) Shows the values of pressure peaks and its locations .

| Injection timing (ATDC) | Pressure peak (bar) | Location (ATDC) |
|--------------------------|----------------------|------------------|
| -12 | 79.0919 | 1.875 |
| -9 | 75.7299 | 4 |
| -6 | 71.628 | 4.625 |
| -3 | 67.8425 | 8 |
| 0 | 63.3401 | 11.25 |

Table (2) In-cylinder pressure peaks & its locations at high load.

The late injection of fuel in the compression stroke or even at TDC leads to a lower pressure peak due to the occurrence of combustion in the expansion stroke. the pressure curve at injection timing (-3 , 0) fall after TDC then begins to rise as a result of late combustion . The same events occurs at the low load (40N.m= 2.5 bar BMEP) fig.(6). Values of peak pressure and their locations are tableted in table (3).

Table (3) In-cylinder pressure peaks & its locations at low load

| Injection timing (ATDC) | Pressure peak (bar) | Location (ATDC) |
|-------------------------|----------------------|------------------|
| -12 | 70.2232 | -0.25 |
| -9 | 68.0373 | 2.125 |
| -6 | 65.1732 | 4.25 |
| -3 | 60.9393 | 7.625 |
| 0 | 52.8173 | 12.375 |

Figure (7) shows the effect of injection timing on the value of the pressure peaks at high load and low load (5 & 2.5 bar BMEP), its shows clearly the decreasing of pressure peaks values when injection timing Approaching to TDC also shows the obvious difference of pressure peaks values at high and low loads .Effect of injection timing on heat released rate at low load is shown in Figure (8), it is noticeable that the retardation of the injection timing causes a reduction in the heat release rate and the combustion phase is shifted towards the expansion stroke.

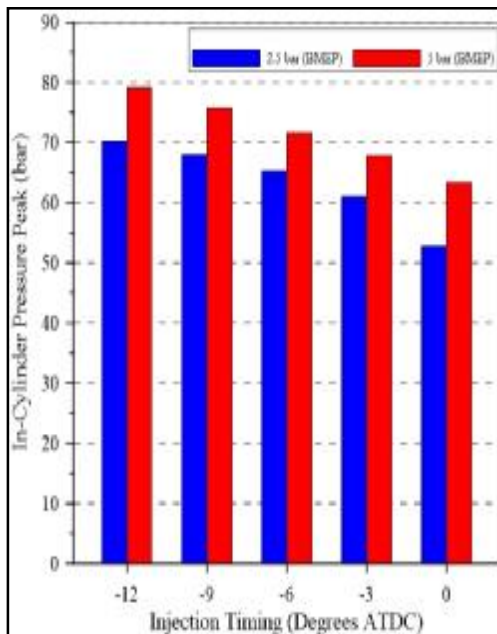


Figure.(7) In-cylinder pressure peak at different injection timing

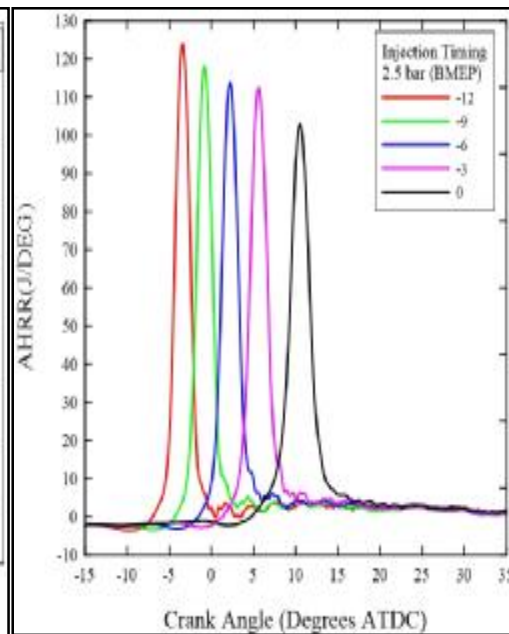


Figure.(8) Apparent heat release rate under low load at different injection timing

Although increasing premixed burn fraction at injection timing (6- ATDC) then (-3 ATDC) and (0 ATDC) as shown in the figure (14) , Which results from increase of delay ignition as shown in the figure (11) , but also that, low temperature at Late injection leads to decrease the heat released rate .At high load heat release rate decreases at injection timing (-12,-9,-6) but increase at (-3,0) as shown in fig (9) , This may be due to increase the ignition delay and therefore the premixed burn fraction is larger at late injection conditions this is clear in figures (11) and (14) , This might be happening due to the increase of combustion temperature at high load.

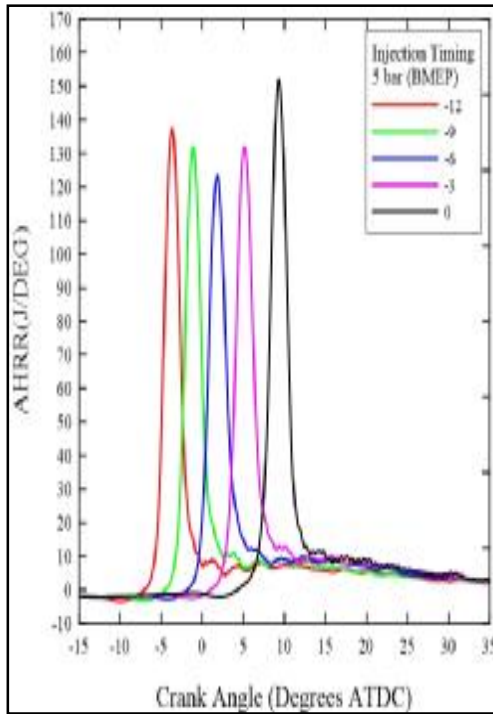


Figure.(9) Apparent heat release rate under high load at different injection timing

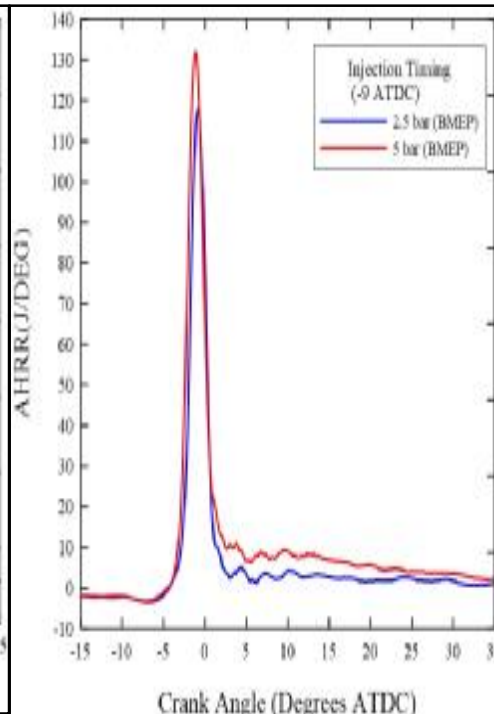


Figure.(10) Apparent heat release rate under high and low load at (-9 ADTC) injection timing

Figure (10) shows the difference between heat released rate peak at high and low load. It is observed that AHRR peak at high load is higher than that at low load in all injection timings .This may be because operation temperatures are higher at high load. Vaporization of fuel will occur more readily than at lower temperatures, reducing the physical component of ID time[13,40,41]. Therefore, it is probable that the observed reduction in ID at higher load is related to the impact of temperature change upon the physiochemical properties of fuel (its higher viscosity, density, heat capacity, and surface tension, reduced vapor pressure, etc.), which make the fuel generally more resistant to vaporization as shown in figure (11) . Figure (12) shows the plot of combustion duration (DOC) with injection timing, the overall DOC was calculated as the difference in the CAD between the EOC and the SOC. The end of combustion (EOC) was determined by considering 90% value of the normalised cumulative heat release rate and it is defined in terms of CAD.

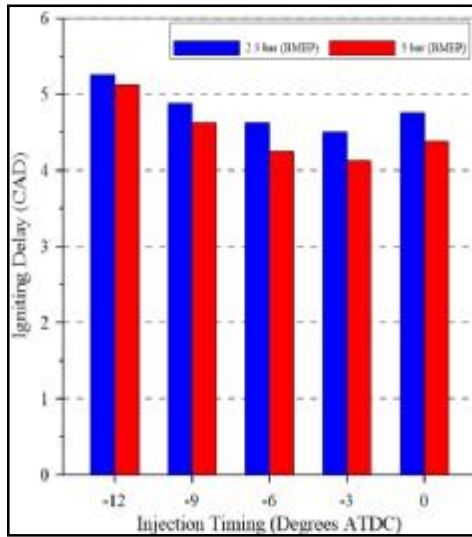


Figure (11) Ignition delay under high and low load

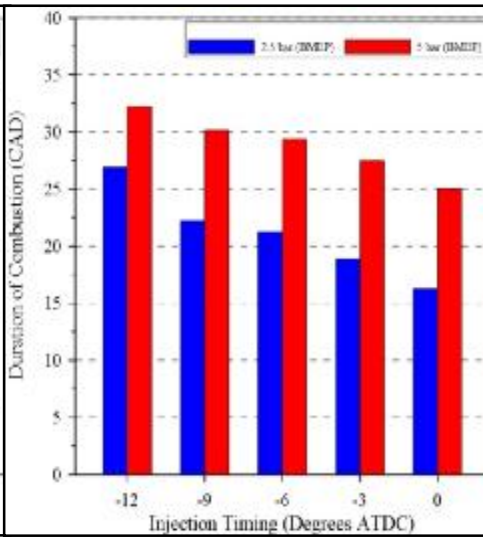


Figure (12) effect of injection timing on

The overall DOC is the sum of premixed and diffusion combustion durations. Within this sum, the change in the premixed DOC remained almost short, therefore the overall DOC inherits the trend of diffusion combustion duration for all cases as shown in fig. (13).

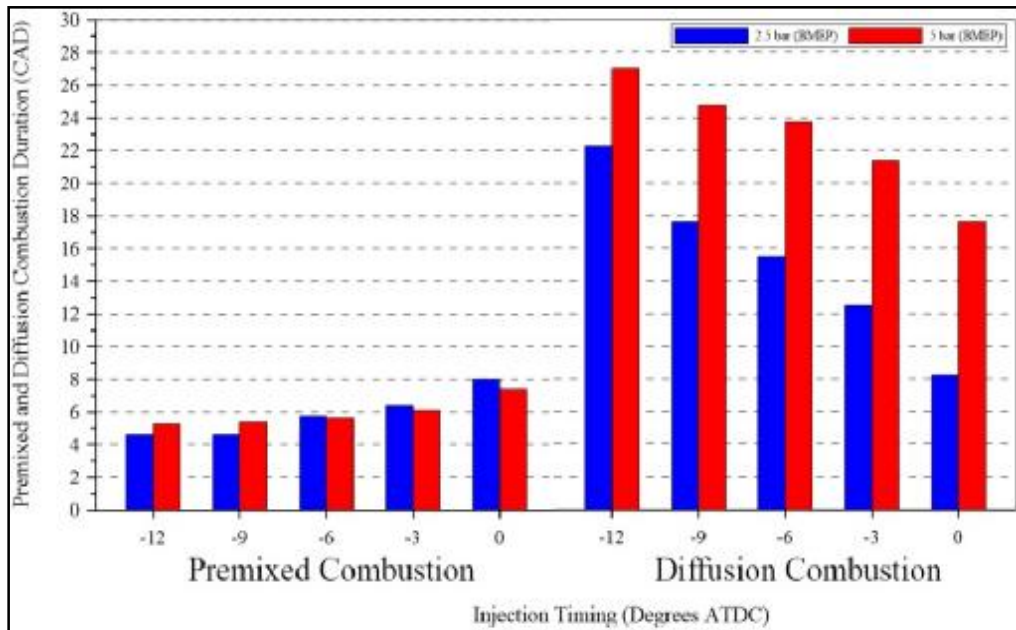


Figure (13) effect of injection timing on duration of premixed and diffusion combustion

It is noticeable that duration of combustion for high load longer than duration of combustion for low load. In order to understand this, Figure (13) provides information about the duration of combustion in the premixed phase as well as in the diffusion phase. The premixed and diffusion combustion duration are distinguished using the second differential of the heat release rate. There is a significant difference between diffusion combustion duration at high load and diffusion combustion duration at low load can be observed ,while there are no noticeable differences between the premixed combustion duration at high load and premixed combustion duration at low load.

Despite shorter premixed burn duration, the magnitude of heat that is released during this phase (mass burn fraction) is higher compared to the magnitude of heat that is released in the diffusion phase fig. (14), As a result of the complete combustion resulting from combustion of premixed fuel –air mixture.

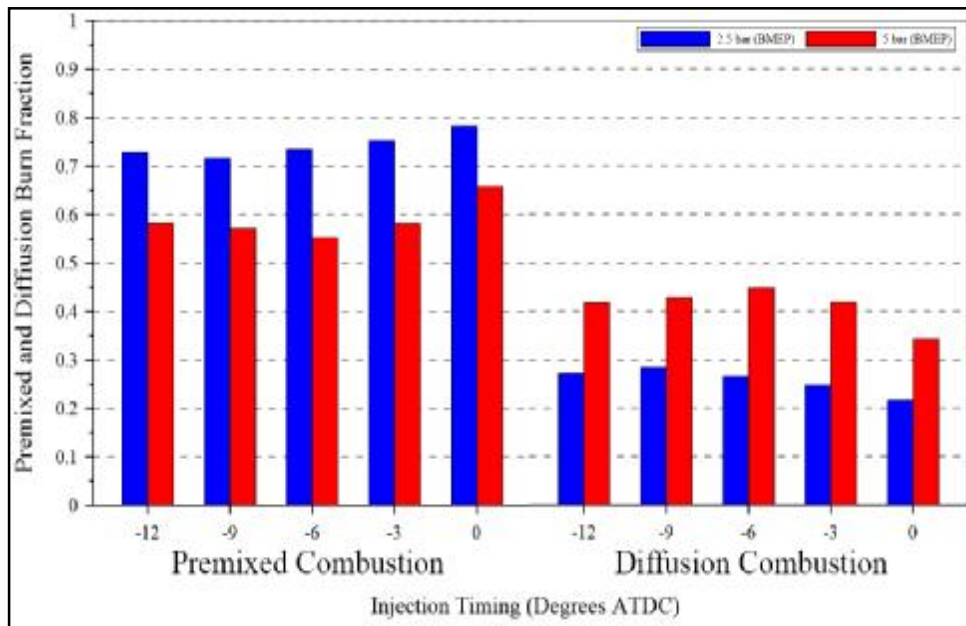


Figure (14) effect of injection timing on premixed and diffusion burn fraction

It is noticeable that the retardation of the injection timing increase the heat released in premixed phase due to the increase of ignition delay and good mixing of mixture.

The Brake Specific Fuel Consumption (BSFC) for different injection timings are shown in fig. (15) , The increase in BSFC at low load is a result of the incomplete combustion of fuel , Therefore, the engine running at low load is considered uneconomic, Effect of injection timing on fuel consumption was limited.

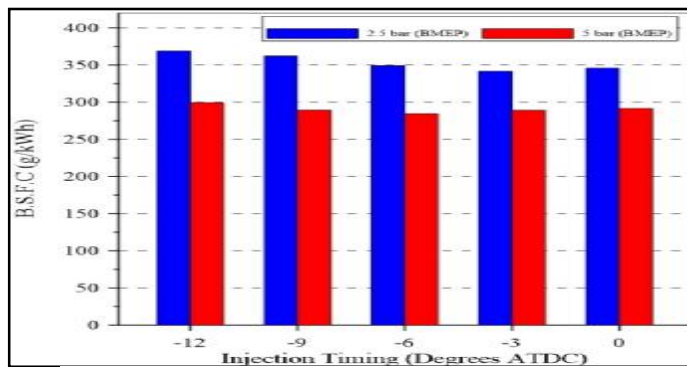


Figure (15) Effect of injection timing on The Brake Specific Fuel on sumption (BSFC) under high and low load

Emission characteristics

Figures (16,17,18,19) show the variation of the nitrogen oxides emissions (NOx), the smoke number (SN), the carbon monoxide emissions (CO) and the total unburnt hydrocarbons emissions (THC) with injection timing .In fig.(16) emissions characteristics of NOx for different injection timing are shown , the retarded injection timing significantly reduces the NOx emissions because of the low in-cylinder temperature resulting from the shift of the combustion into the expansion stroke. As the difference of Noxemissions between high and low-load due to the difference of temperature in combustion chamber . The NOx formation during combustion mainly depends on the Zeldowich mechanism where formation reactions are more intensive in a high temperature environment leading to higher NOx emissions. The highest cylinder temperature occurs during the premixed combustion phase where the formation of NOx is dominant.

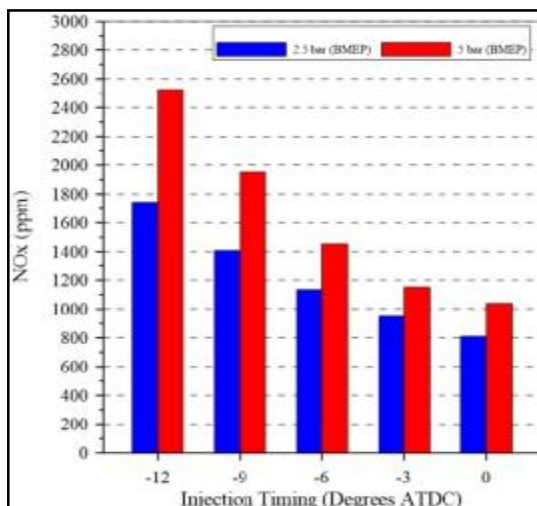


Figure (16)Effect of injection timing on NOx emissions under high and low load

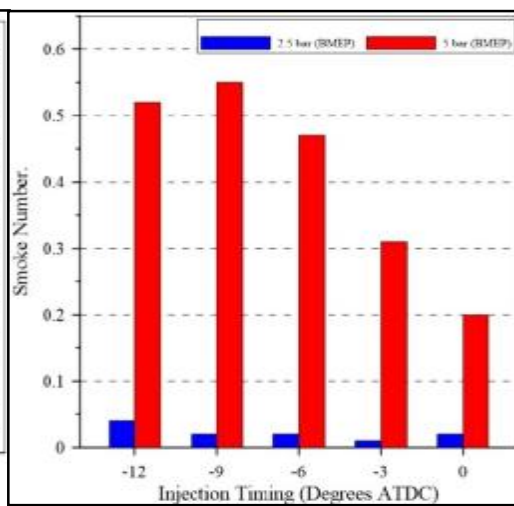


Figure (17) Effect of injection timing on smoke number under high and low load

Fig. (17) Shows the measured smoke number at different injection timings. We can clearly note the huge difference in soot emissions between high load and low-load for all timings, This difference results from the large difference in the amount of diffusion combustion (diffusion burn fraction) between high and low-load, as shown in Figure(14).The heat release rate analyses are helpful in understanding NOx and soot emissions variations for different conditions. A lower magnitude of heat released in the premixed phase, may lead to lower NOx emissions. On the other hand, longer duration of the diffusion combustion phase leads to higher soot emissions. Furthermore, retarding the injection timing produces more heat in the premixed phase as shown in fig.(14) , thus it can be suggested that soot emissions could be lower at late fuel injection timing as shown in fig (18).late injection led to dramatic change in the mode of combustion as compared with conventional diesel combustion, where late injection lead to semi low temperature combustion (LTC) at high load and to completely low temperature combustion (LTC) at low load where both soot and NOx emissions tend to reduced simultaneously.

Fig.(18) shows the variation of (CO) emissions at different fuel injection timings . The effect of the retarded injection timing at low load causes higher increase of (CO) emissions , As mentioned above , (CO) emissions are formed as a result of incomplete combustion, mainlydue to the combustion taking place at low temperature in the expansion stroke. Moreover, the spray-wall impingement could be much greater for the injection of fuel at TDC. This effect was not clear at high load due to the high temperature of the combustion chamber at different conditions.

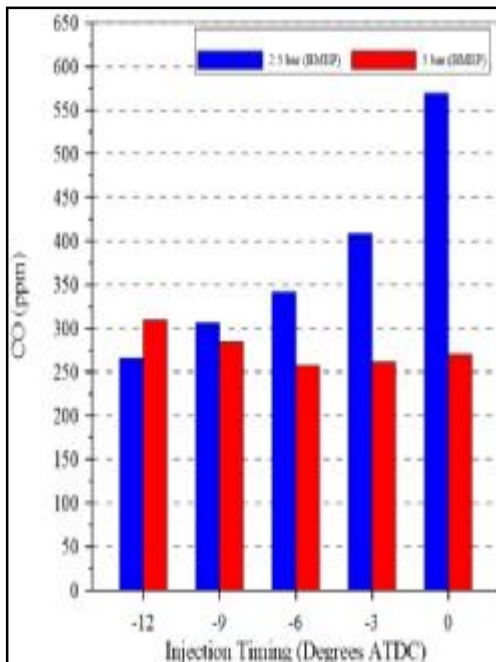


Figure (18) Effect of injection timing on carbon monoxide emissions under high and low load

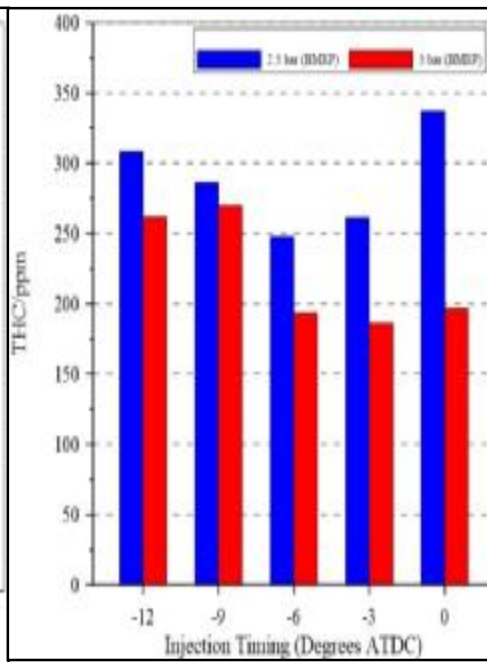


Figure (19) Effect of injection timing on (THC) emissions under high and low load

The effect of fuel injection timings on (THC) emissions shown in fig (19), HC emissions are the result of incomplete combustion in which some hydrocarbons are not fully oxidized. In this respect, HC emissions are closely linked to CO emissions since they are both caused by low quality combustion ,The noted difference between the THC emitted at high load and low load is obviously due to better combustion at high load caused by increase in the temperature .As injection advances THC emission is increased which could be a result of lower charge density at the time of injection which leads to increased spray penetration and ultimately sprays wall impingement, referred to as wall wetting. This is responsible for the increase in the level of unburned fuel. THC emission can also increase due to the presence of very lean mixture caused by over-mixing due to the longer ignition delay period.

CONCLUSIONS

- 1-The retardation of the injection timing leads to increase the ignition delay and therefore the premixed burn fraction is larger at late injection conditions, and this explains the characteristics of combustion and emissions at late injection.
- 2-When running the engine at high load, Increase the premixed burn fraction leads to increase the rate of heat released at late injections.
- 3- Increase premixed burn fraction lead to increase in temperature and thus increasing NOx emissions and reducing soot emissions.
- 4- The diffusion burn fraction at high load is higher than that at low load, which ,leads to significant increase of soot emissions compared to those at low load.
- 5- Late injection can causes to change the combustion mode to semi low temperature combustion (LTC) at high load and to completely low temperature combustion (LTC) at low load where both soot and NOx emissions tend to reduced simultaneously.
- 6- (CO) and (THC) emissions are formed as a result of incomplete combustion, mainly due to the combustion taking place at low temperature in the expansion stroke.
- 7- THC emissions can be increase at advanced injection timing due to lower charge density and also increases due to the presence of very lean mixture caused by over-mixing due to the longer ignition delay period.

Acknowledgment

The experimental work of this research has been in Centre for Advanced Power train and Fuels Research (CAPF), School of Engineering and Design, Brunel University, London , UK

NOMENCLATURE

| | |
|-----------------|------------------------------------|
| AHRR | Apparent heat release rate |
| ATDC | After top dead centre |
| BMEP | Brake mean effective pressure |
| CI | Compression ignition |
| CO | Carbon monoxide |
| CO ₂ | Carbon dioxide |
| C _p | Specific heat at constant pressure |
| C _v | Specific heat at constant volume |
| DBF | Diffusion burn fraction |
| EGR | Exhaust Gas Recirculation |

| | |
|-----------------|------------------------------|
| EOC | End of combustion |
| EOPMB | End of premixed burn |
| HSDI | High speed direct injection |
| ID | Ignition delay |
| NO | Nitrogen monoxide |
| NO ₂ | Nitrogen dioxide |
| NO _x | Nitric oxides |
| PM | Particulate matter |
| PMBF | Premixed burn fraction |
| SOC | Start of combustion |
| SOI | Start of injection |
| SN | Smoke number |
| THCs | Total hydrocarbons |
| ULSD | Ultra-low sulfur diesel fuel |

REFERENCE

- [1]NO_x: How Nitrogen Oxides Affect the Way We Live and Breathe; Report No. EPA-456/F-98-005; United States Environmental Protection Agency, Office of Air Quality Planning and Standards: Research Triangle Park, NC, 1998.
- [2]Nitrogen Oxides (NO_x), Why and How They Are Controlled; Report No. EPA-456/F-99-006R, United States Environmental Protection Agency, Office of Air Quality Planning and Standards: Research Triangle Park, NC, 1999.
- [3]Glassman, I.; Yetter, R. A. Combustion, 4th ed.; Elsevier Academic Press: Burlington, MA, 2008.
- [4]Ban-Weiss, G. A.; Chen, J. Y.; Buchholz, B. A.; Dibble, R. W. A numerical investigation into the anomalous slight NO_x increase when burning biodiesel; A new (old) theory. *Fuel Process. Technol.* 2007, 88, 659–667.
- [5]Turns, S. R. An Introduction to Combustion: Concepts and Applications, 2nd ed.; Tata McGraw-Hill: New Delhi, India, 2012.
- [6]Modeling Pollutant Formation. In ANSYS Fluent, Fluent 6.3 Documentation; Fluent Inc.: Lebanon, NH, 2006; Chapter 20.
- [7]D. M. Peirce, N. S. I. Alozie, D. W. Hatherill, and L. C. Ganippa . Premixed Burn Fraction: Its Relation to the Variation in NO_x Emissions between Petro- and Biodiesel. *Energy Fuels* 2013, 27, 3838–3852
- [8]Fenimore, C. P. Formation of nitric oxide in premixed hydrocarbon flames. *Proc. Combust. Inst.* 1971, 13, 373–380.
- [9]Miller, J. A.; Bowman, C. T. Mechanism and modeling of nitrogen chemistry in combustion. *Prog. Energy Combust. Sci.* 1989, 15, 287–338.
- [10]Bowman, C. T. Kinetics of pollutant formation and destruction in combustion. *Prog. Energy Combust. Sci.* 1975, 1, 33–45.
- [11]Konnov, A. A. Implementation of the NCN pathway of prompt- NO formation in the detailed reaction mechanism. *Combust. Flame* 2009, 156, 2093–2105.
- [12]Xi, J., and Zhong, B., 2006. Soot in Diesel Combustion Systems. *Chemical Engineering Technology*, Vol. 29, No. 6
- [13]Heywood, J.B., 1988. *Internal Combustion Engine Fundamentals* McGraw-Hill Science Engineering
- [14]Suzuki, H., Koike, N., Ishii, H., Odaka, M., 1997. Exhaust Purification of Diesel Engines by Homogeneous Charge with Compression Ignition Part 1: Experimental

Investigation of Combustion and Exhaust Emission Behavior Under Pre-Mixed Homogeneous Charge Compression Ignition Method. SAE Paper 970313

[15] Kittelson, D.B., Watts, W.F., Johnson, J.P., Rowntree, C.J., Goodier, S.P., Payne, M.J., Preston, W.H., Warrens, C.P., Ortiz, M., Zink, U., Goersmann, C., Twigg, M.V., Walker, A.P., 2006. Driving Down On-Highway Particulate Emissions. SAE Paper 2006-01-0916

[16] Senda, J., Ikeda, M., Yamamoto, M., Kawaguchi, B., Fujimoto, H., 1999. Low Emission Diesel Combustion System by Use of Reformulated Fuel with liquefied CO₂ and n-Tridecane. SAE Paper 1999-01-1136

[17] Kawano, D., Senda, J., Kawakami, K., Shimada, A., Fujimoto, H., 2001. Fuel Design Concept for Low Emission in Engine Systems -2nd report Analysis of Combustion Characteristics for the mixed fuels. SAE Paper 2001-01-1071

[18] Adomeit, P., Pischinger, S., Becker, M., Rohs, H., Greis, A., Grünefeld, G., 2006. Potential Soot and CO Reduction for HSDI Diesel Combustion Systems. SAE Paper 2006-01-1417

[19] Miyamoto, N., Ogawa, H., Nurun, N.M., Obata, K., Arima, T., 1998. Smokeless, Low NO_x, High Thermal Efficiency, and Low Noise Diesel Combustion with Oxygenated Agents as Main Fuel. SAE Paper 98-05-06

[20] Kitamura, T., Ito, T., Senda, J., and Fujimoto, H., 2001. Detailed Chemical Kinetic Modeling of Diesel Spray Combustion with Oxygenated Fuels. SAE Paper 2001-01-1262

[21] Xu, Y., Lee, C.F., 2006. Study of Soot Formation of Oxygenated Diesel Fuels Using Forward Illumination Light Extinction (FILE) Technique. SAE Paper 2006-01-1415

[22] Kwanhee Choi, Juwon Kim, Ahyun Ko, Cha-Lee Myung, Simsoo Park, Jeongmin Lee. Size-resolved engine exhaust aerosol characteristics in a metal foam particulate filter for GDI light-duty vehicle. *Journal of Aerosol Science* 57 (2013) 1–13

[23] Sara Pinzi, Paul Rounce, José M. Herreros, Athanasios Tsolakis, M. Pilar Dorado. The effect of biodiesel fatty acid composition on combustion and diesel engine exhaust emissions. *Fuel* 104 (2013) 170–182.

[24] Karavalakis, G., Bakeas, E., Stournas, S., 2010. An Experimental Study on the Impact of Biodiesel Origin and Type on the Exhaust Emissions from a Euro 4 Pick-up Truck. SAE Paper 2010-01-2273

[25] Kawano, D., Mizushima, N., Ishii, H., Goto, Y., Iwasa, K., 2010. Exhaust Emission Characteristics of Commercial Vehicles Fuelled with Biodiesel. SAE Paper 2010-01-2276

[26] Juwon Kim, Kwanhee Choi, Cha-Lee Myung, Youngjae Lee, Simsoo Park. Comparative investigation of regulated emissions and nano-particle characteristics of light duty vehicles using various fuels for the FTP-75 and the NEDC mode. *Fuel* 106 (2013) 335–343

[27] Sergey Ushakov, Harald Valland, Vilmar Esøy. Combustion and emissions characteristics of fish oil fuel in a heavy-duty diesel engine. *Energy Conversion and Management* 65 (2013) 228–238

[28] Kuhnert, S., Wagner, U., Spicher, U., Haas, S.F., Gabel, K., Kutschera, I., 2010. Influence of Injection Nozzle Hole Diameter on Highly Premixed and Low Temperature Diesel Combustion and Full Load Behavior. SAE Paper 2010-01-2109

- [29]D.C. Rakopoulos. Heat release analysis of combustion in heavy-duty turbocharged diesel engine operating on blends of diesel fuel with cottonseed or sunflower oils and their bio-diesel. *Fuel* 96 (2012) 524–534
- [30]SalihManasra, Dieter Brueggemann. Effect of Injection Pressure and Timing on the In-Cylinder Soot Formation Characteristics of Low CR Neat GTL-Fueled DI Diesel Engine. SAE Paper 2011-01-2464
- [31]Seung Hyun Yoon, Chang Sik Lee. Effect of biofuels combustion on the nanoparticle and emission characteristics of a common-rail DI diesel engine. *Fuel* 90 (2011) 3071–3077
- [32]M. Mani , G. Nagarajan. Influence of injection timing on performance, emission and combustion characteristics of a DI diesel engine running on waste plastic oil. *Energy* 34 (2009) 1617–1623
- [33]C.A.J. Leermakers, B. Van den Berge, C.C.M. Luijten, L.M.T. Somers and L.P.H. de Goey. Gasoline-Diesel Dual Fuel: Effect of Injection Timing and Fuel Balance. SAE Paper 2011-01-2437.
- [34]Rakesh Kumar Maurya, Avinash Kumar Agarwal. Effect of Start of Injection on the Particulate Emission from Methanol Fuelled HCCI Engine. SAE Paper 2011-01-2408.
- [35]Á Díez, H Zhao, T Carrozzo, A E Catania and E Spessa. Development of a high-speed two-colour system and its application to in-cylinder diesel combustion temperature and soot measurements with split injections. *Proceedings of the Institution of Mechanical Engineers, Part D: Journal of Automobile Engineering* 2012 226: 684
- [36]Mohammad Reza Herfatmanesh and Hua Zhao. Experimental investigation of effects of dwell angle on fuel injection and diesel combustion in a high-speed optical CR diesel engine. *Proceedings of the Institution of Mechanical Engineers, Part D: Journal of Automobile Engineering* 2013 227: 246.
- [37]Asish K Sarangi, Colin P Garner, Gordon P McTaggart-Cowan, Martin H Davy, EmadWahab and Mark Peckham. The effects of split injections on high exhaust gas recirculation low-temperature diesel engine combustion. *International Journal of Engine Research* 2013 14: 68
- [38]José M Desantes, José M Luján, BenjamínPla and José A Soler. On the combination of high-pressure and low-pressure exhaust gas recirculation loops for improved fuel economy and reduced emissions in high-speed direct-injection engines. *International Journal of Engine Research* 2013 14: 3
- [39]L. Labecki, A. Cairns, J. Xia, A. Megaritis, H. Zhao, L.C. Ganippa. Combustion and emission of rapeseed oil blends in diesel engine. *Applied Energy* 2012.02.026
- [40]Vaughn, T.; Hammill, M.; Harris, M.; Marchese, A. J. Ignition delay of bio-ester fuel droplets. SAE Technical Paper 2006-01-3302 .
- [41]Obert, E. F. *Internal Combustion Engines and Air Pollution*; Harper and Row Publishers: New York, 1973.

Appendix A

A photograph of the engine and smoke meter



Appendix B

Kistler 6125A pressure transducer



Appendix C

a photograph of Horiba Gas Analyser

